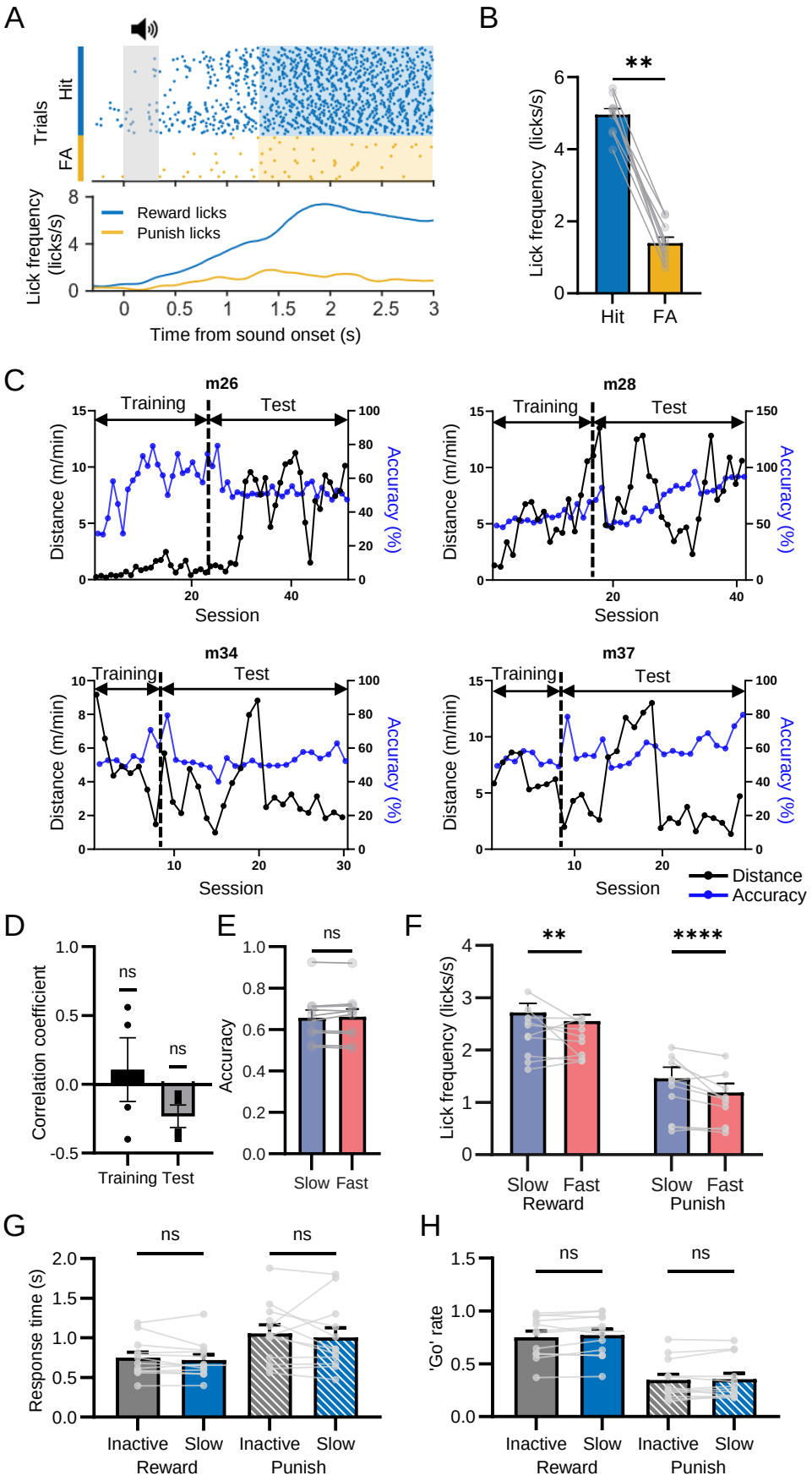
A
Trials
Hit
FA
Lick frequency (licks/s)
Reward licks
Punish licks
Time from sound onset (s)
B
**
Lick frequency (licks/s)
Hit
FA
C
m26
m28
m34
m37
Training
Test
Distance (m/min)
Accuracy (%)
Session
Distance
Accuracy
D
Correlation coefficient
ns
Training Test
E
Accuracy
Slow Fast
F
Lick frequency (licks/s)
**
****
Slow Fast
Reward
Punish
G
Response time (s)
Inactive Slow
Reward
Punish
H
'Go' rate

Figure S1. Additional decision-making performance data, related to Figure 1.
(A) Raster plot of licks and average traces of lick frequency during reward (Hit) and punishment (FA) trials for an example session aligned on sound cue onset. Grey shaded area is the time when the sound cue is present. Blue and yellow shaded areas are the time window that the reward or punishment is given. (B) Comparison of average lick frequency in response window between reward (Hit) and punishment (FA) trials. Error bars: mean ± SEM, **p<0.01(p=0.002), Wilcoxon signed rank test, n = 10 mice. (C) Total walking distance and test accuracy during training and test periods for all four mice. We used spearman correlation to compare the correlation between walking distance and accuracy during training and test. (D) Correlation coefficients of walking distance and test accuracy for each mouse during training and test sessions. Error bar: mean ± SEM, training: p=0.6250, test: p=0.1250, One sample Wilcoxon test, n = 4 mice. (E) Task accuracy comparison between slow and fast speed trials. Error bars: mean ± SEM, p=0.70, Wilcoxon signed rank test, n = 10 mice. (F) Lick frequency comparison between slow and fast speed trials in response to reward cues or punishment cues across all sessions. Error bars: mean ± SEM, **p<0.01, ****p<0.0001 (reward: p=0.0022, punish: p<0.0001), two-way ANOVA with repeated measure Bonferroni correction, n = 10 mice. (G) Response time comparison between inactive and slow speed trials in response to reward cues or punishment cues across all sessions in TRE-EGFP expressing control mice from the Cal-Light experiments. Error bars: mean ± SEM, ns (all p>0.05 for reward and punish trials), two-way ANOVA with repeated measure Bonferroni correction, n = 12 mice. (H) Go response rate comparison between inactive and slow speed trials in response to reward cues (Hit / (Hit+Miss)) or punishment cues (FA / (FA+CR)) across all sessions in TRE-EGFP expressing control mice from the Cal-Light experiments. Error bars: mean ± SEM, ns (all p>0.05 for reward and punish trials), two-way ANOVA with repeated measure Bonferroni correction, n = 12 mice. from control mice Cal-Light experiment

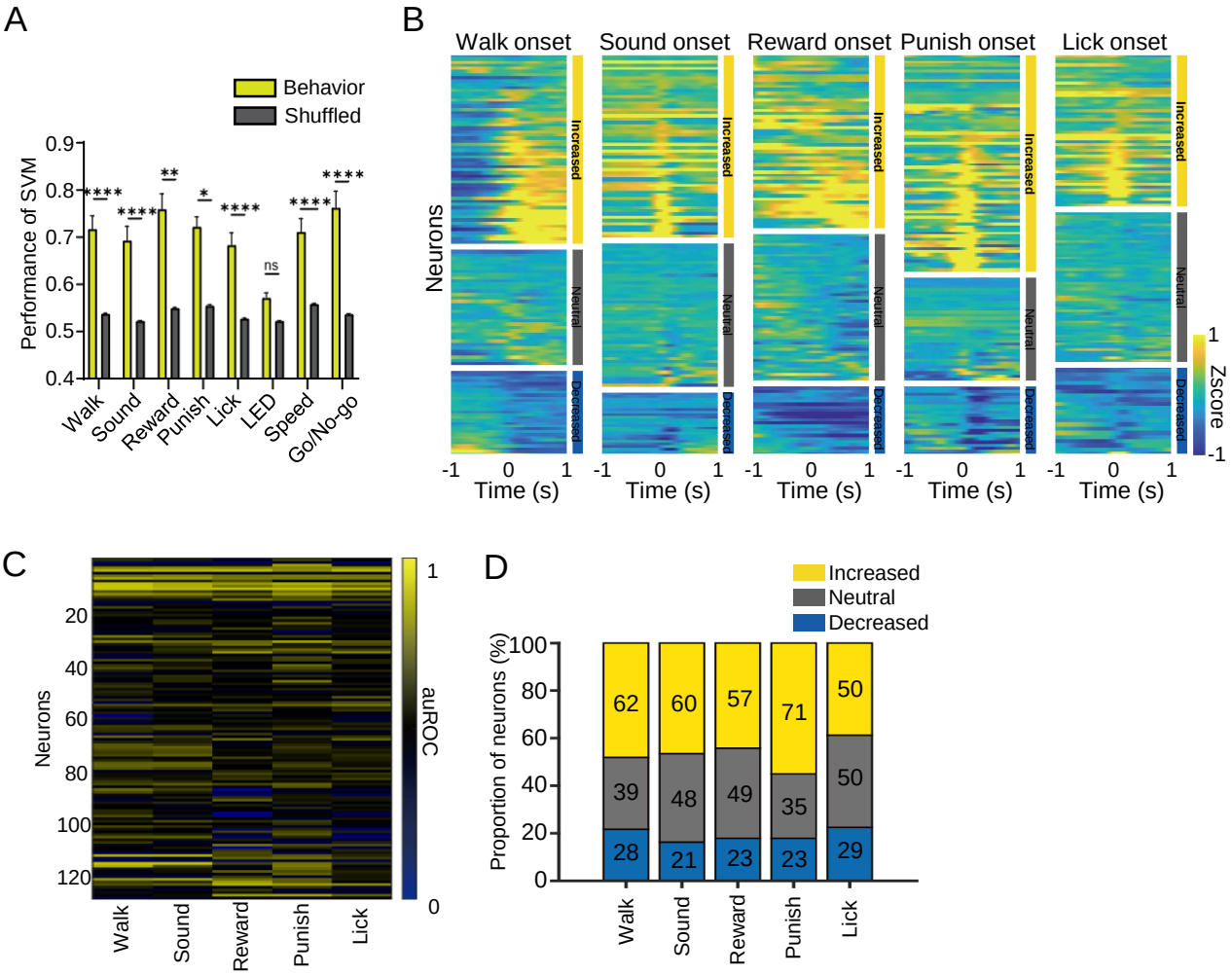

Figure S2. MLR neuronal responses to various event types, related to Figure 2.
(A) Performances of binary SVM decoders. Decoders were trained to classify targeted event and baseline for each event type using population activity. Error bars: mean + SEM, *p<0.05, **p<0.01, ***p<0.005, ****p<0.001 (walk: p=0.0005, sound: p=0.0005, reward: p=0.0093, punish: p=0.0122, lick: p=0.0015, led: p=0.65, speed: p=0.00097, go/no-go: p=0.0005), Wilcoxon signed rank test, n = 11 sessions. (B) Z-scored average responses of MLR neurons grouped into increased (auROC > 95% of shuffled distribution), decreased (auROC < 5% of shuffled distribution), and neutral as defined by Area Under the ROC Curve (auROC) for the onset of each event type. (C) Raster plot of auROC of all MLR neurons for walk, lick, sound cue, reward and punishment onsets (D) Fraction of neurons that were increased, neutral, and decreased responsive cells for each event type.

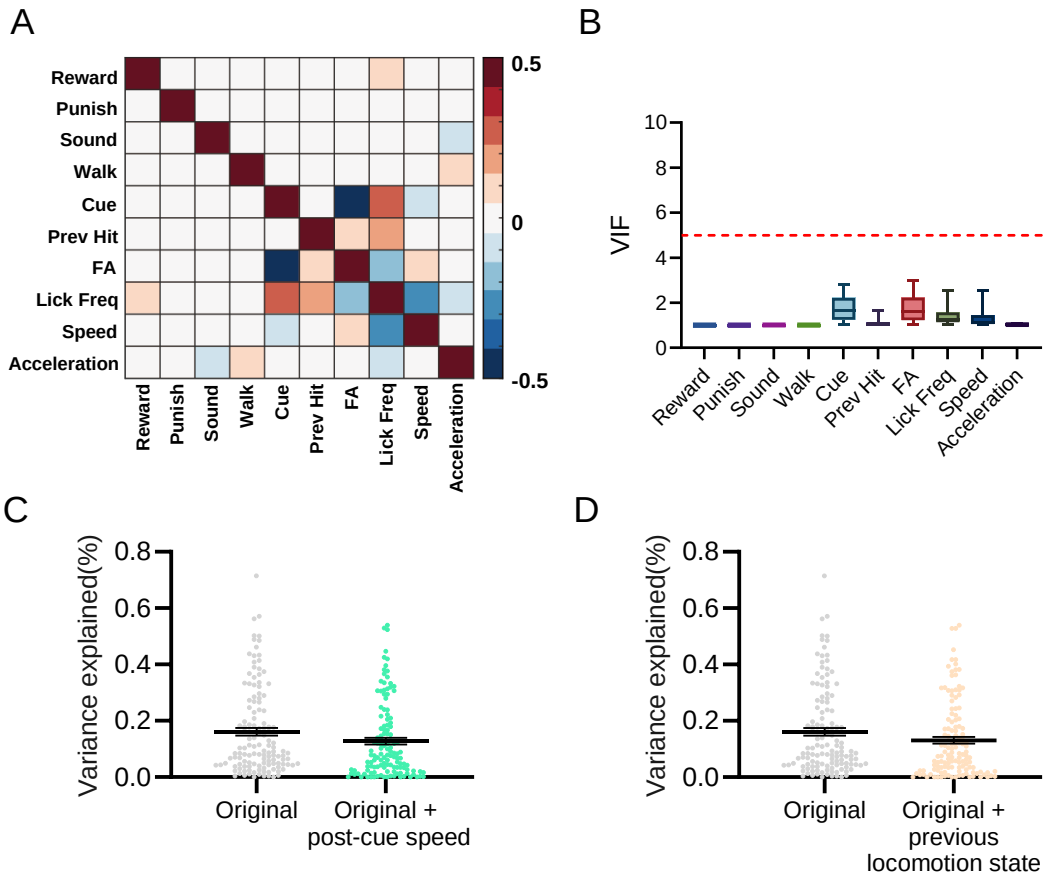

Figure S3. Multicollinearity assessment of behavioral variables in GLM analysis and comparison of encoding models with additional variables, related to Figure 2.
(A) Similarity matrix for average Pearson's correlation coefficient between pairs of behavioral variable traces from all sessions. (B) The variance inflation factors (VIFs) for each of behavioral variable traces corresponding to other 9 components. Error bars: mean ± SEM, All $p<0.0001$, One sample Wilcoxon test to test less than 5, n = 17 sessions. (C) Comparison of explained variance between the original encoding model using all behavioral variables and an encoding model with an additional variable (100ms post-cue speed), Error bars: mean ± SEM, ns, $p>0.05$, one-sided paired t-test (original < additional model) (D) Comparison of explained variance between the original encoding model using all behavioral variables and an encoding model with an additional variable (locomotor state of previous trial; slow or fast), Error bars: mean ± SEM, ns, $p>0.05$, one-sided paired t-test (original < additional model)

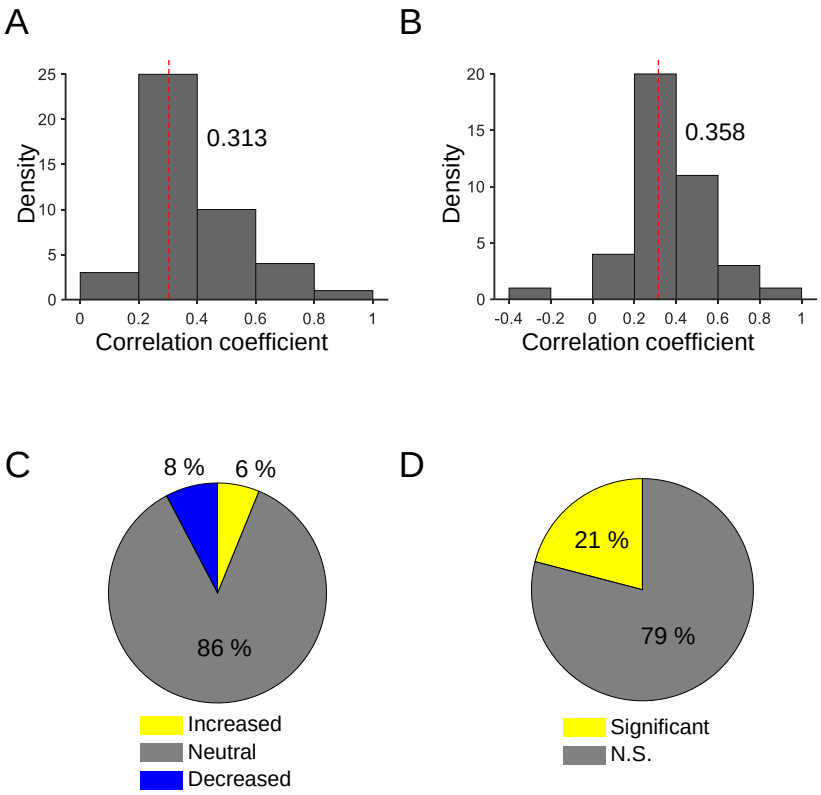

Figure S4. Additional characterization of MLR neuronal responses to various event types using SVM and ROC analysis, related to Figure 2.
(A) Correlation between trial-by-trial neuronal activity across consecutive trials. Histogram showing the distribution of correlation coefficients between sustained activity in trial n (measured during the last 1 s of the response window) and pre-cue activity in trial n+1 (measured during the 1 s preceding cue onset). The mean correlation coefficient is 0.313. (B) Histogram showing the distribution of correlation coefficients between sustained activity in trial n (measured during the last 1 s of the response window) and the post-stimulus interval activity in trial n+1 (measured during the post-stimulus interval). The mean correlation coefficient is 0.358. (C) Predictive power of trial n sustained activity for trial n+1 choice (ROC analysis). Pie chart illustrates the proportion of neurons whose sustained activity during the last 1 s of trial n significantly encoded the choice (Go vs. No-go) of the subsequent trial (n+1), as determined by ROC analysis. Neurons were categorized into increased (auROC > 95% of shuffled distribution), decreased (auROC < 5% of shuffled distribution), or neutral groups. (D) Predictive power of trial n sustained activity for trial n+1 choice (SVM analysis). Pie chart illustrates the proportion of neurons whose sustained activity significantly encoded the choice of the subsequent trial, determined by SVM analysis using single-neuron activity. Neurons were classified as significant if their decoding accuracy exceeded the 95th percentile of the shuffled distribution.

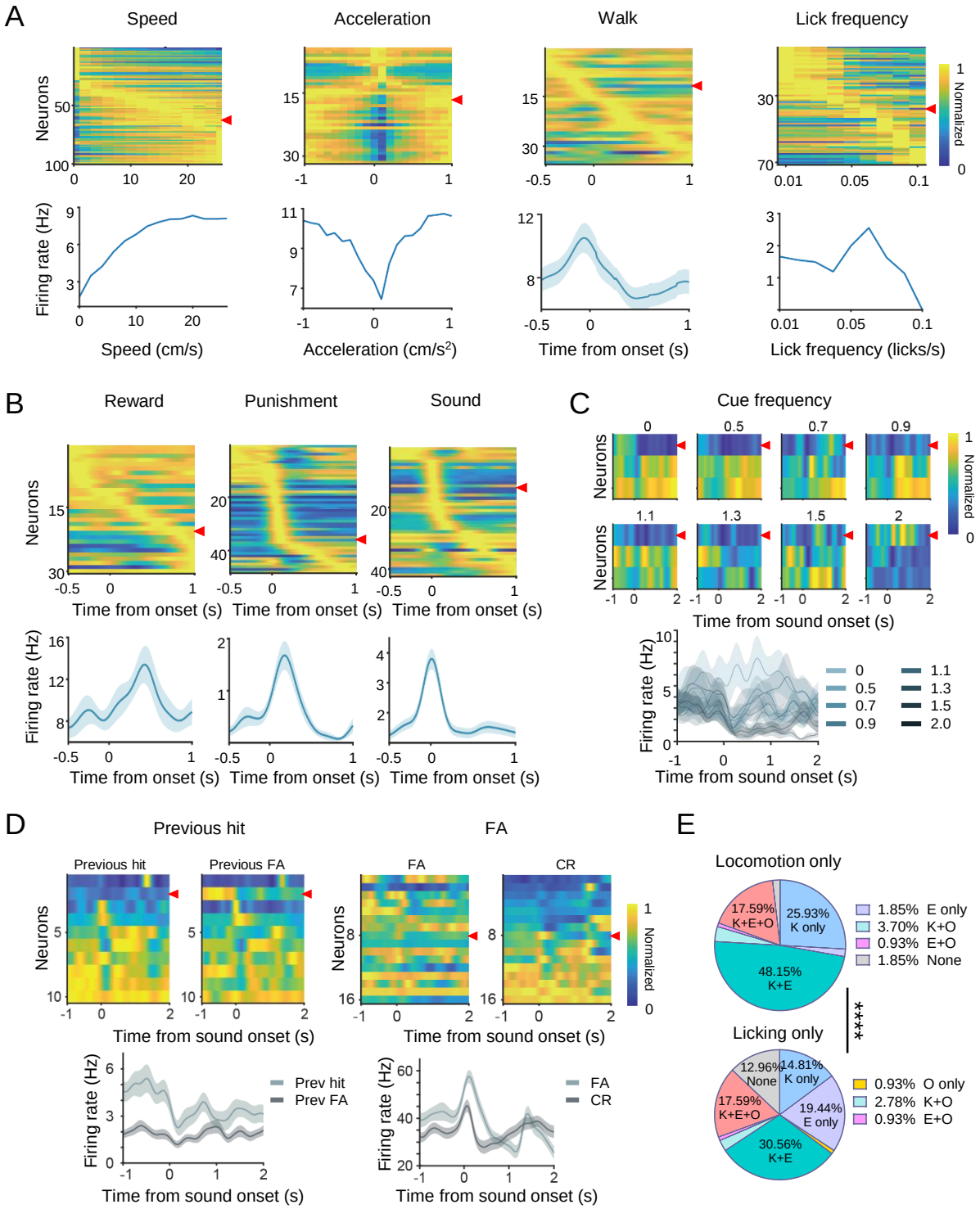

Figure S5. Detailed dynamics and encoding distributions of MLR neuronal responses to kinematic and non-kinematic variables, related to Figure 2.

(A) Neural response in association with the kinematic behavior variables (speed, acceleration, walk onset, and lick frequency) for significantly modulated neurons by those variables. The top panels are normalized average raster for all significantly modulated neurons by each variable, and the bottom panels are average firing rate of representative neuron. Red arrows indicate representative neurons. Error bars, mean ± SEM. (B) Same as (A), but with neurons which modulated by non-kinematic event type variables. Error bars, mean ± SEM. (C) Same as (A), but with neurons which modulated by whole trial type cue frequency variable. Cue frequency is presented as relative octave level (0 to 2.0) of actual sound frequency (8 to 32 kHz). Error bars, mean ± SEM. (D) Same as (A), but with neurons which modulated by non-kinematic whole trial type variables (Previous hit, FA). Error bars, mean ± SEM. (E) Frequency distribution of multiplexing pattern of neurons separated by consideration of locomotion (top) and licking behaviors as kinematic variables (bottom). ****p<0.0001, Chi-square test.

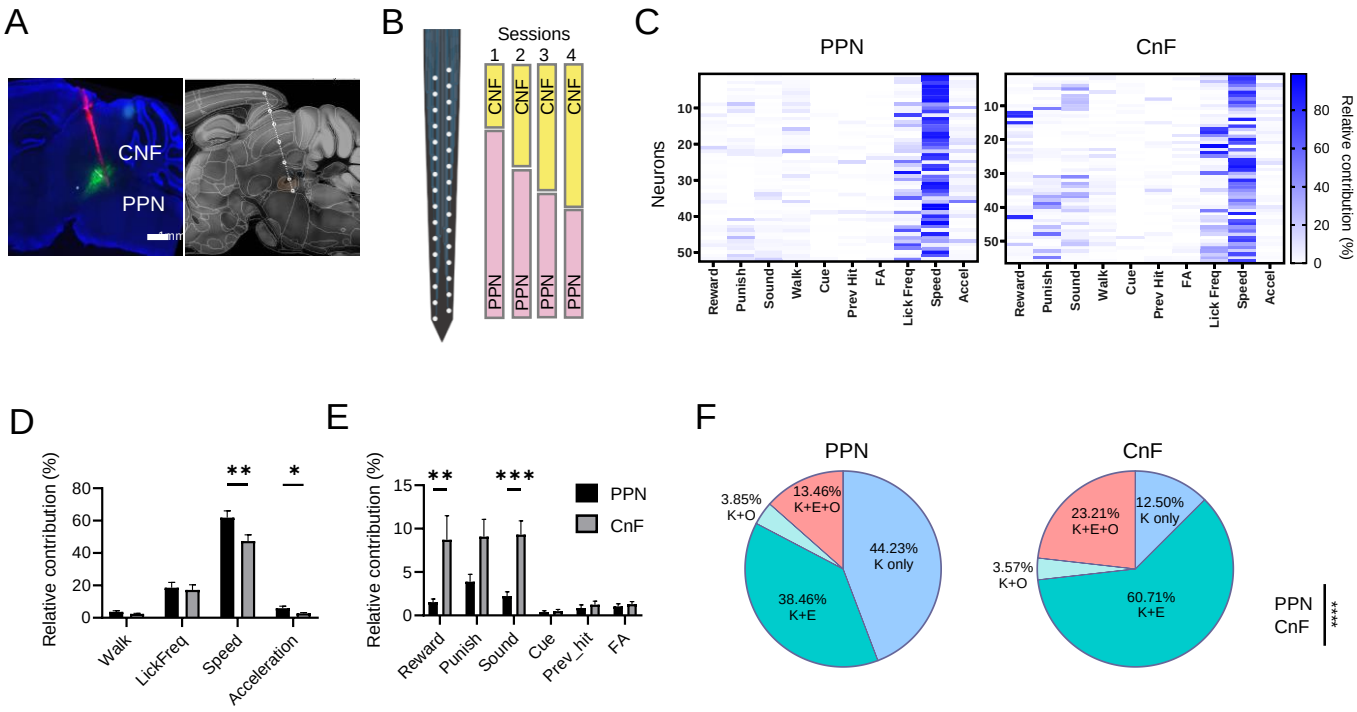

Figure S6. Different multiplexing patterns between PPN and CnF, related to Figure 2.
(A) Histology image of silicon probe insertions targeting PPN and CnF. (B) Dimensions of multichannel electrodes during 4 example sessions. (C) Raster plot showing relative contribution of each behavioral variable to explain variance for neurons in PPN and CnF. (D) Comparison of relative contribution of kinematic variables between PPN and CnF neurons. *p<0.05, **p<0.01 (speed: p=0.003, acceleration: p=0.03), Mann-Whitney test. (E) Comparison of relative contribution of non-kinematic variables between PPN and CnF neurons. Error bars: mean + SEM, **p<0.01, ***p<0.001 (reward: p =0.002, punish: p=0.051, sound: p=0.0006), Mann-Whitney test. (F) Frequency distribution of multiplexing patterns in PPN and CnF. ****p<0.0001, Chi-square test (PPN: n = 52, CnF: n = 56).

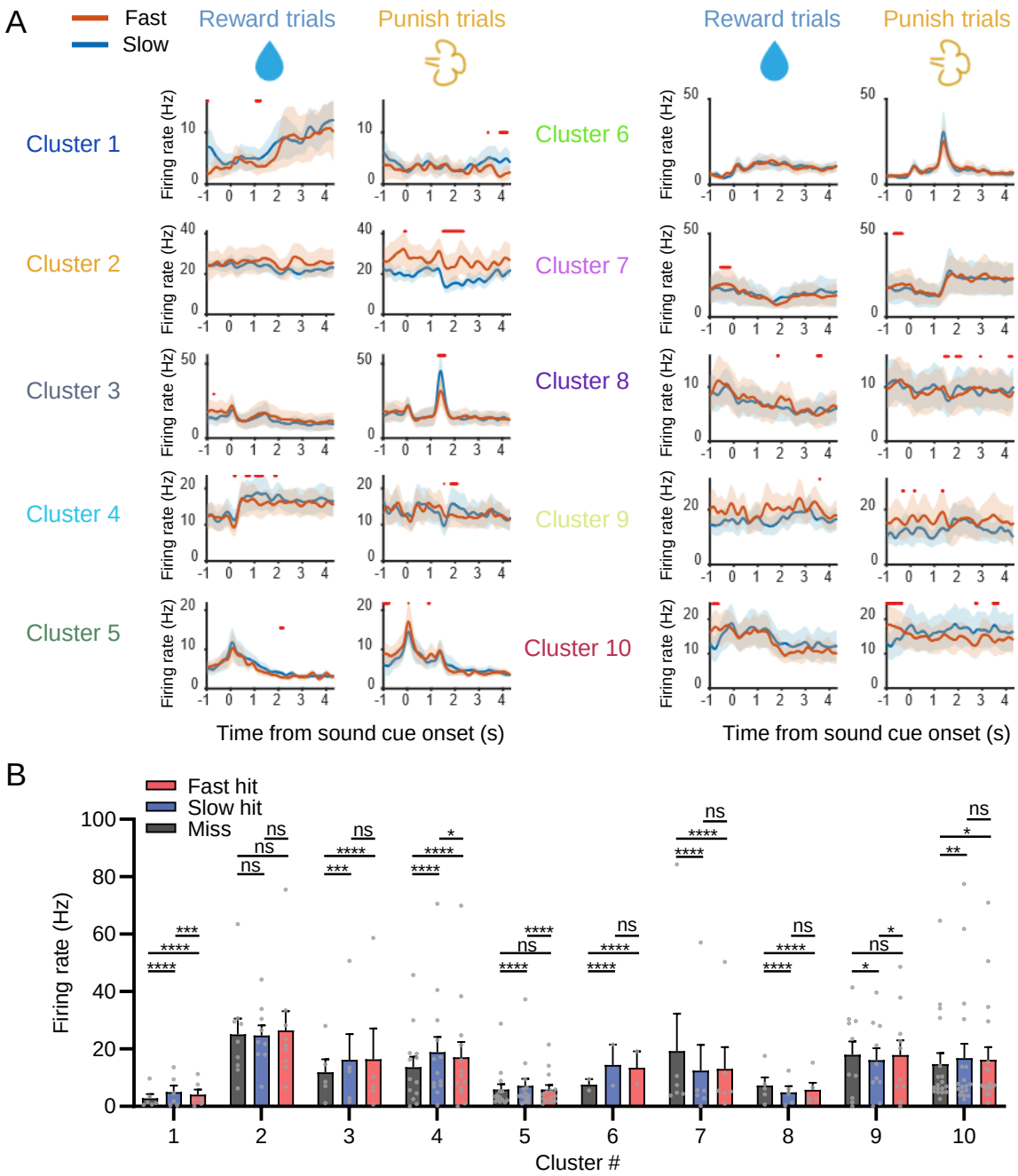

Figure S7. Activity dynamics of MLR functional clusters, related to Figure 3.
(A) Average firing rate traces of all 10 clusters during 4 types of trials (slow walking + reward, fast walking + reward, slow walking + punishment, fast walking + punishment) aligned to sound cue onset. Red dots indicate statistical comparison between lines: p<0.05, Wilcoxon signed rank test. (B) Comparison of average firing rates during the post-stimulus interval in miss trials, reward trials with slow walking speed, and fast walking speed for all clusters. Grey dots represent individual data points. Error bars: mean + SEM, ns, p>0.05; *p<0.05; **p<0.01; ***p<0.001; ****p<0.0001; two-way ANOVA with repeated measure Bonferroni correction performed for each clusters.

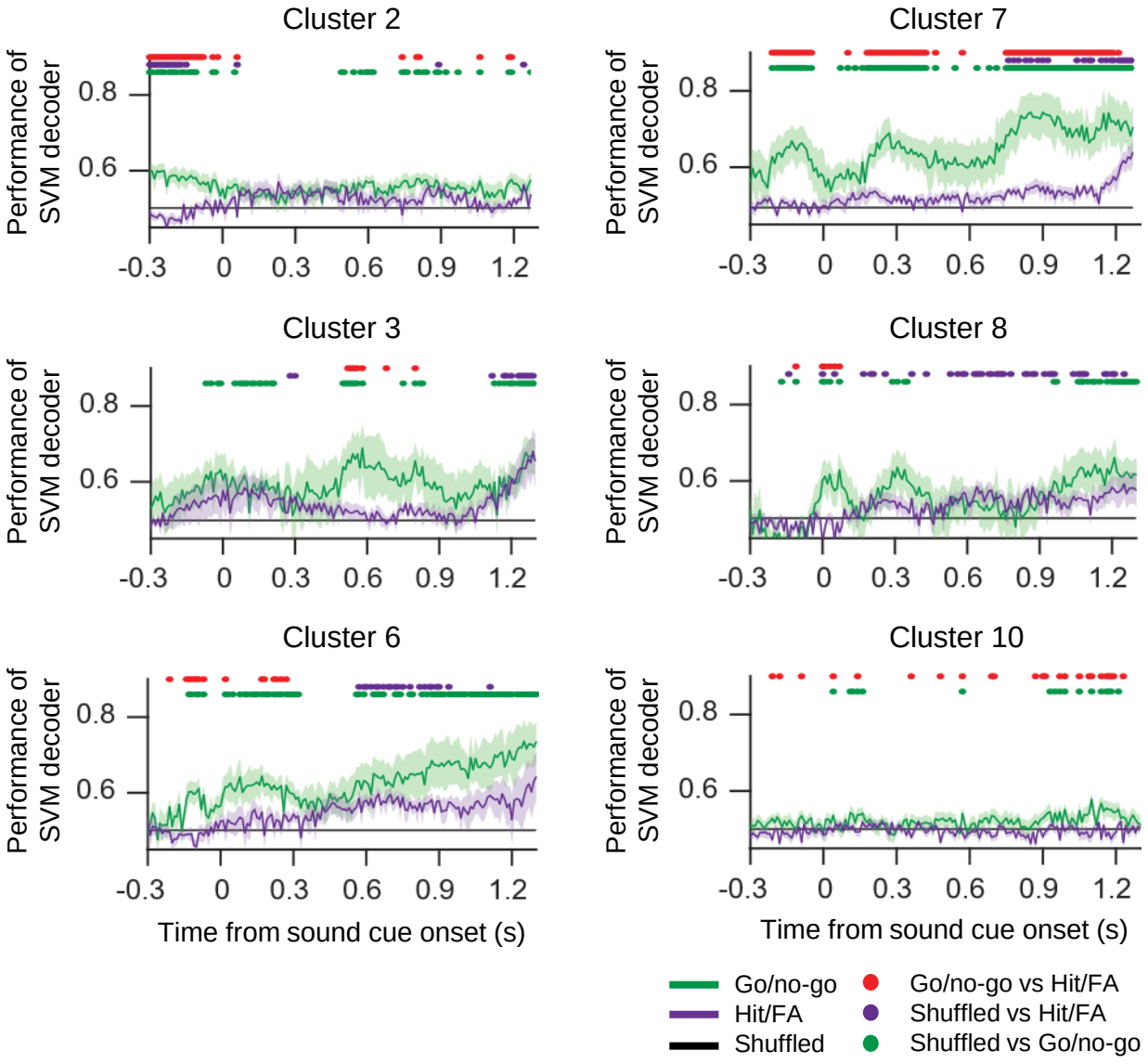

Figure S8. Temporal dynamics of choice and outcome encoding across MLR functional clusters, related to Figure 3.

Average performance traces of binary SVM decoders of neurons in cluster 2, 3, 6, 7, 8,10 from -0.3 to 1.3 s after the onset of sound cue. Decoders were trained to classify between 'go' and 'no-go' trials (green line), or between hit or false alarm trials (purple line) using the firing rate of each neuron at every time bin. Error bars: mean ± SEM, Red, purple, and green dots indicate statistical comparison between lines: $p<0.05$, one-sample Wilcoxon test.

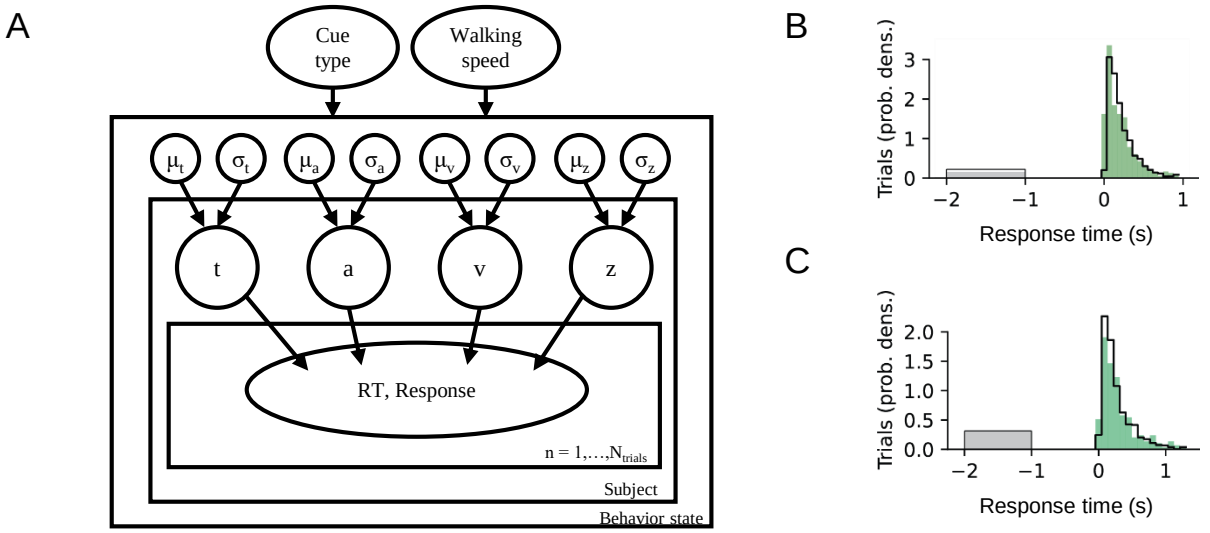

Figure S9. Detailed drift diffusion model analysis of movement dependent decision-making, related to Figure 4.

(A) Simplified graphical model showing hierarchical drift diffusion model parameters. (B) Example RT distribution of whole trials with slow-speed condition from 17 sessions. Black lines indicate simulated data from 'v' model with best fit, and colored background is observed data distribution. Positive RT means go response and negative RT means occurrence of no-go response. (C) Same as (B), but of trials with fast-speed condition.

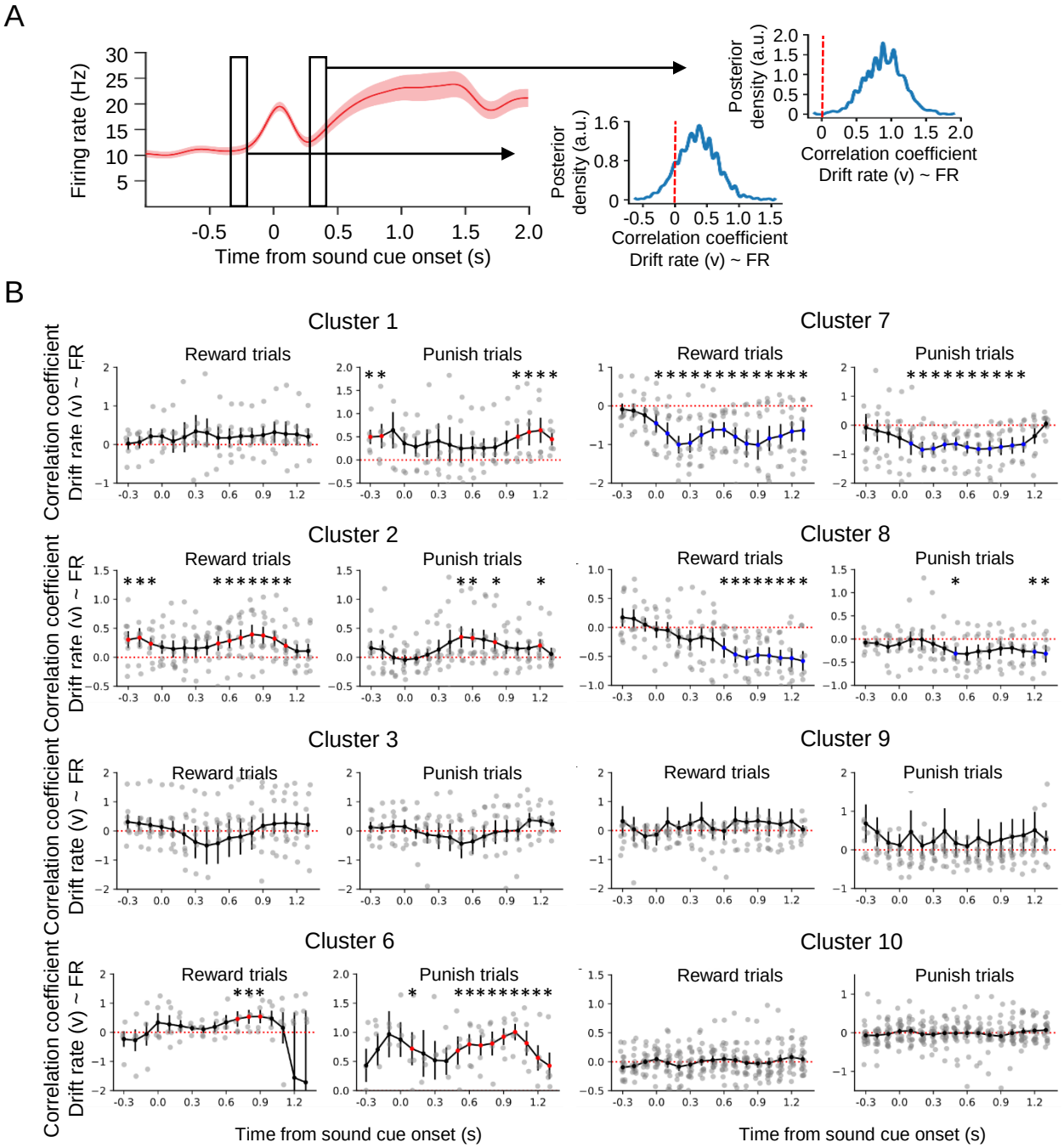

Figure S10. Regression analysis for measuring correlation between neuronal firing rates and drift rates in four clusters, related to Figure 4.

(A) Schematic of regression analysis of individual neuron's firing rates against drift rate (v) within the time bins from -0.3 to 1.3 s after the onset of sound cue (averaged over 100ms interval). (B) Summary of regression analysis between firing rates of individual neurons in all clusters except cluster 4 and 5, and drift rate (v), within the time bins from -0.3 to 1.3 s after the onset of sound cue in both reward and punishment trials. Error bars: mean + SEM, *p<0.05, one-sample Wilcoxon test.

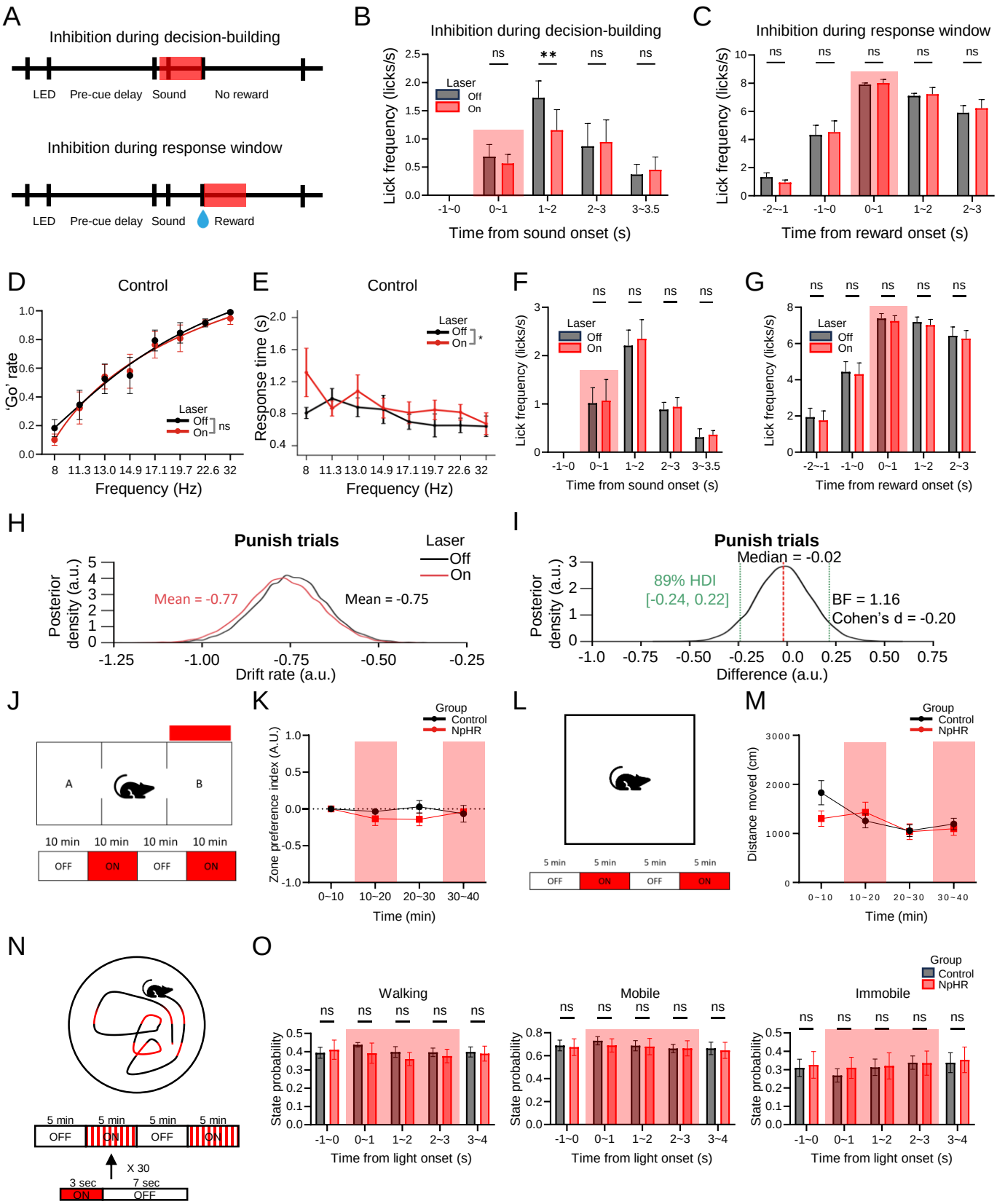
A
Inhibition during decision-building
LED
Pre-cue delay
Sound
No reward
Inhibition during response window
LED
Pre-cue delay
Sound
Reward
B
Inhibition during decision-building
Lick frequency (licks/s)
Laser
Off
On
ns
**
ns
ns
-1~0
0~1
1~2
2~3
3~3.5
Time from sound onset (s)
C
Inhibition during response window
Lick frequency (licks/s)
ns
-2~-1
-1~0
0~1
1~2
2~3
Time from reward onset (s)
D
Control
'Go' rate
Laser
Off
On
ns
Frequency (Hz)
E
Control
Response time (s)
Laser
Off
On
*
Frequency (Hz)
F
Lick frequency (licks/s)
Laser
Off
On
Time from sound onset (s)
G
Lick frequency (licks/s)
Laser
Off
On
Time from reward onset (s)
H
Punish trials
Laser
Off
On
Posterior density (a.u.)
Mean = -0.77
Mean = -0.75
Drift rate (a.u.)
I
Punish trials
Median = -0.02
89% HDI
[-0.24, 0.22]
BF = 1.16
Cohen's d = -0.20
Posterior density (a.u.)
Difference (a.u.)
J
A
B
10 min
OFF
ON
K
Group
Control
NpHR
Zone preference index (A.U.)
Time (min)
L
5 min
OFF
ON
M
Group
Control
NpHR
Distance moved (cm)
Time (min)
N
5 min
OFF
ON
X 30
3 sec
7 sec
O
Walking
Mobile
Immobile
Group
Control
NpHR
State probability
Time from light onset (s)

Figure S11. Additional data with optoinhibition of Cal-Light-labeled MLR neurons, related to Figure 5.

(A) Schematic of inhibition timing during the decision-building period (top) and during the response window (bottom). (B) Lick frequency during “laser off” (black) and “laser on” (red) trials, measured from –1 s to 3.5 s relative to sound onset (inhibition during the decision-building period; red shaded box). Error bars: mean ± SEM, **p<0.01 at 1-2 s (ns, p>0.05 elsewhere), paired t-test across time bins, n = 4 mice. (C) Lick frequency during “laser off” (black) and “laser on” (red) trials, measured from –2 s to 3 s relative to sound onset (inhibition during the response window; red shaded box). Error bars: mean ± SEM, ns (all p>0.05 across time bins), paired t-test across time bins, n = 4 mice. (D-G) Same analyses as Figure 5D, E, G, and H, but performed in control mice expressing TRE-EGFP instead of TRE-NpHR-EYFP. (D) Error bars: mean ± SEM, ns (p>0.05), two-way ANOVA, main effect of Laser: F(1,315) = 0.32, n = 5 mice. (E) Error bars: mean ± SEM, *p<0.05, two-way ANOVA, main effect of Laser: F(1,59) = 6.17, n = 5 mice. (F) Error bars: mean ± SEM, ns (all p>0.05 across time bins), paired t-test across time bins, n = 5 mice. (G) Error bars: mean ± SEM, ns (all p>0.05 across time bins), paired t-test across time bins, n = 5 mice. (H) Posterior density plots of drift rate (v) estimated from a drift-diffusion model in which laser stimulation was allowed to modulate all core parameters (v, a, z, and t), shown separately for punishment trials. (I) Posterior density plots of the difference in drift rate (v) between laser off and laser on conditions for punishment trials. The median difference is indicated by the vertical red dotted line, and the green dotted lines represent the 89% Highest Density Interval (HDI), which summarizes the most credible region of the posterior distribution,. Bayes factors (BF), computed relative to a Region of Practical Equivalence (ROPE = [−0.07, 0.07], corresponding to approximately 5–10% of the baseline drift-rate magnitude from the vanilla model), indicate the presence of a moderate effect in reward trials (BF = 3 – 6, moderate evidence; BF < 3, weak evidence). Cohen's d quantifies a standardized effect size, with absolute values above 0.8 conventionally considered large. (J) Schematic of the real-time place preference test. (K) Zone preference index comparison between control and NpHR groups (inhibition during 10-20 and 30-40 min; red shaded box). Error bars: mean ± SEM, ns (all p>0.05 across time bins), paired t-test across time bins, Control: n = 5, NpHR: n = 4 mice. (L) Schematic of the open field test. (M) Distance moved comparison between control and NpHR groups (inhibition during 10-20 and 30-40 min; red shaded box). Error bars: mean ± SEM, ns (all p>0.05 across time bins), unpaired t-test across time bins, Control: n = 5, NpHR: n = 4 mice. (N) Schematic of the pulse-mode inhibition test. (O) Comparison of state probability changes of walking, mobile, and immobile behavior states between control and NpHR groups. Red shaded area indicates the inhibition period. Error bars: mean ± SEM (ns, p>0.05), unpaired t-test across time bins, Control: n = 5, NpHR: n = 4 mice.